Chapter 3

Theory of quadrupole mass spectrometers

In this chapter, the theory of ion motions in a time-varying electric-quadrupole field is developed. The motions of ions in RF-QMF and ITMS is described with the solutions of Mathieu equation which was originally developed by Mathieu[23] in his investigation of the motions of a vibrating elliptical membrane. Later on, McLachlan examined in detail[24].

First, we summarize the Mathieu equation and its solutions. Then the application to the description of ion motions in RF-QMF is presented. The motions of ions in a three dimensional quadrupole fields are given in the last part of this chapter.

3.1 Mathieu equation

The Mathieu equation[23, 24] is expressed as follows:

$$\frac{\mathrm{d}^2u}{\mathrm{d}\xi^2}+\left[a_u-2q_u\cos 2(\xi-\xi_0)\right]u(\xi)=0 \qquad (3.1.1)$$

where a_u and q_u are real constants. In the application of this equation to RF-QMF or ITMS, the function $u(\xi)$ is one of the coordinates of moving ions in the (x,y,z) cartesian coordinate system, while the variable ξ is related to the phase of the RF field.

A general solution can be written by a linear combination of two independent solutions of $u_1(\xi)$ and $u_2(\xi)$ in such a way that

$$u(\xi)=\Gamma u_1(\xi)+\Gamma' u_2(\xi)\ . \qquad (3.1.2)$$

The coefficients Γ and Γ' in the solution depend upon the initial conditions of the ion position $u(0)$, the initial velocity $(du/dt)_{t=0}$ and the initial RF phase ξ_0. From Floquet's theorem[25], we know there exists a solution in the form of

$$u(\xi) = e^{\mu\xi}\psi(\xi) \ . \tag{3.1.3}$$

In this solution, μ is a constant and $\psi(\xi)$ has a period of π. The functions $u_1(\xi)$ and $u_2(\xi)$ are in general either even or odd functions. We put them as follows:

$$u_1(\xi) = u_1(-\xi) \qquad \text{and} \qquad u_2(\xi) = -u_2(-\xi) \ . \tag{3.1.4}$$

Thus the solution can be written in the following form:

$$u(\xi) = \Gamma e^{\mu\xi}\psi(\xi) + \Gamma' e^{-\mu\xi}\psi(-\xi) \ . \tag{3.1.5}$$

According to Fourier's theorem, a periodic function may be expressed as an infinite sum of exponential terms, namely

$$\psi(\xi) = \sum_{n=-\infty}^{\infty} C_{2n} \exp(2ni\xi) \qquad \text{and} \qquad \psi(-\xi) = \sum_{n=-\infty}^{\infty} C_{2n} \exp(-2ni\xi) . \tag{3.1.6}$$

The coefficients C_{2n} in the above functions describe the amplitudes of ion motion, and depend only on the parameters a_u and q_u. Substituting eq.(3.1.6) into eq.(3.1.5), we obtain the following expression:

$$u(\xi) = \Gamma e^{\mu\xi} \sum_{n=-\infty}^{\infty} C_{2n} \exp(2ni\xi) + \Gamma' e^{-\mu\xi} \sum_{n=-\infty}^{\infty} C_{2n} \exp(-2ni\xi) . \tag{3.1.7}$$

The constant μ is a complex number defined by

$$\mu = \alpha + i\beta \ , \tag{3.1.8}$$

and it is related to the parameters a_u and q_u as given below[22,24];

$$a_u = \mu^2 + \frac{1}{2(\mu^2-1)} q_u^{\ 2} + \frac{(5\mu^2+7)}{32(\mu^2-1)^3(\mu^2-4)} q_u^{\ 4}$$

$$+\frac{(9\mu^4+58\mu^2+29)}{64(\mu^2-1)^5(\mu^2-4)(\mu^2-9)}q_u^{\,6}+\cdots . \qquad (3.1.9)$$

The constant μ is referred to as the *characteristic exponent* because it determines the type of solution of the Mathieu equation. There exist two types of solution. The first type is a stable solution which remains finite as ξ increases. The other type is unstable and increases without limit with the increase of ξ. The solution given by eq.(3.1.7) becomes unstable when $\alpha \neq 0$, since one of the terms of $\exp(\mu\xi)$ or $\exp(-\mu\xi)$ increases to infinity. Therefore, only the solution with α =0 is stable. Then, if we substitute $\mu=i\beta$ into eq.(3,1,7), it reduces to

$$u(\xi)=\Gamma\sum_{n=-\infty}^{\infty}C_{2n}\exp[(2n+\beta)i\xi]+\Gamma'\sum_{n=-\infty}^{\infty}C_{2n}\exp[-(2n+\beta)i\xi]. \qquad (3.1.10)$$

With the identity of $\exp(i\theta)=\cos\theta+i\sin\theta$, the above stable solution can be modified into

$$u(\xi)=\mathrm{A}\sum_{n=-\infty}^{\infty}C_{2n}\cos(2n+\beta)\xi+\mathrm{B}\sum_{n=-\infty}^{\infty}C_{2n}\sin(2n+\beta)\xi \qquad (3.1.11)$$

with the definitions for coefficients A and B as

$$\mathrm{A}=(\Gamma+\Gamma') \qquad \text{and} \qquad \mathrm{B}=i(\Gamma-\Gamma'). \qquad (3.1.12)$$

Therefore, Eq.(3-1-11) becomes a real stable solution only in the following case:

$$\Gamma=\frac{1}{2}(\mathrm{A}-i\mathrm{B}) \qquad \text{and} \qquad \Gamma'=\frac{1}{2}(\mathrm{A}+i\mathrm{B}). \qquad (3.1.13)$$

From the relationship of a_u and q_u with the constant μ given by eq.(3.1.9), any sets of a_u and q_u which yields μ in a pure imaginary form of $\mu=i\beta$ are allowable for stable solutions. Such allowable sets of a_u and q_u for stable solutions are given by points (a_u, q_u) in the shaded areas in Fig.3-1. It should be noted that the stability region is symmetric with respect to q_u =0, since the parameter a_u is expanded with even powers of q_u in eq.(3.1.9). Therefore, the parameter q_u can be regarded as a positive value ($q_u > 0$) for convenience.

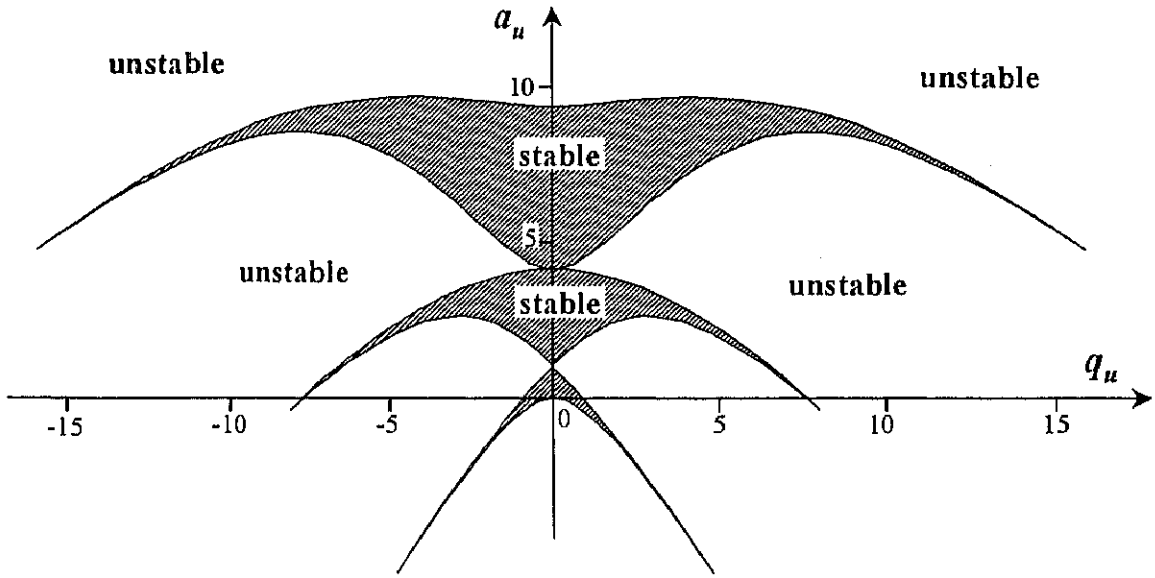

Fig.3-1 Mathieu stability diagram in one dimension. The suffix u can be read x or y. The shaded regions give the values of a_u and q_u for stable solutions.

3.2 Quadrupole mass filter

3.2.1 The equation of ion motion and its solution

The ideal field required for RF-QMF is a two-dimensional electric quadrupole field as shown in Fig.3-2. This field can be generated in the space surrounded by four electrodes with the cross sections of hyperbolic boundaries. Because of the difficulty in the machining of the electrodes, the hyperbolic boundaries are usually approximated with circular ones. A schematic arrangement of RF-QMF consisting of four rod electrodes was already shown in Fig.2-5(a).

A voltage of Φ_0 is applied to a pair of electrodes placed on the x-axis, face-to-face with each other. Another voltage of opposite polarity $-\Phi_0$ is applied to another pair of electrodes on the y-

axis as shown in Fig.3-2. Each voltage of $\pm \Phi_0$ is a superposition of a DC voltage of U and an RF voltage of $V_{RF}\cos\Omega t$ as follows:

$$\Phi_0 = U - V_{RF}\cos\Omega t \qquad \text{and} \qquad -\Phi_0 = -(U - V_{RF}\cos\Omega t) \ . \tag{3.2.1}$$

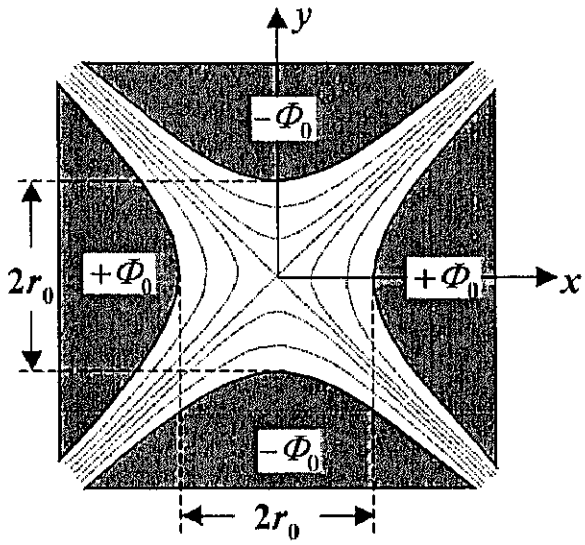

Fig.3-2 Hyperbolic electrodes with equipotential contours in an ideal QMF.

The electric potential Φ for the electrode configuration in Fig.3-2 is given by

$$\Phi(x,y) = \frac{\Phi_0}{r_0^{\,2}}(x^2 - y^2) = \frac{U - V_{RF}\cos\Omega t}{r_0^{\,2}}(x^2 - y^2) \ . \tag{3.2.2}$$

Then the electric fields are derived as

$$E_x = -\frac{\partial\Phi(x,y)}{\partial x} = -2\frac{U - V_{RF}\cos\Omega t}{r_0^{\,2}}x \tag{3.2.3a}$$

and

$$E_y = -\frac{\partial\Phi(x,y)}{\partial y} = +2\frac{U - V_{RF}\cos\Omega t}{r_0^{\,2}}y \ . \tag{3.2.3b}$$

We can immediately write equations of the ion motions in this field for an ion with mass m and charge q. The explicit forms are

$$m\frac{d^2x(t)}{dt^2} = -2q\frac{U - V_{RF}\cos\Omega t}{r_0^{\,2}}x \tag{3.2.4a}$$

$$m\frac{d^2y(t)}{dt^2} = +2q\frac{U - V_{RF}\cos\Omega t}{r_0^{\,2}}y \tag{3.2.4b}$$

$$m\frac{d^2z(t)}{dt^2} = 0\ . \tag{3.2.4c}$$

Here, we introduce the following change of the variable:

$$\Omega t = 2\xi\ . \tag{3.2.5}$$

Equations (3.2.4a), (3.2.4b) and (3.2.4c) now can be written as

$$\frac{d^2x(\xi)}{d\xi^2} + \frac{8q}{m\Omega^2 r_0^{\,2}}\left[U - V_{RF}\cos 2\xi\right]x(\xi) = 0 \tag{3.2.6a}$$

$$\frac{d^2y(\xi)}{d\xi^2} - \frac{8q}{m\Omega^2 r_0^{\,2}}\left[U - V_{RF}\cos 2\xi\right]y(\xi) = 0 \tag{3.2.6b}$$

$$\frac{d^2z(\xi)}{d\xi^2} = 0\ . \tag{3.2.6c}$$

Thus, if we define the parameters containing U and V_{RF} in such a way that

$$a_x = \frac{8qU}{\Omega^2 m r_0^{\,2}} = -a_y \tag{3.2.7}$$

and

$$q_x = \frac{4qV_{RF}}{\Omega^2 m r_0^{\,2}} = -q_y\ , \tag{3.2.8}$$

the motions of the ions in x- and y-directions are both described by the following Mathieu equation:

$$\frac{d^2u}{d\xi^2}+\left[a_u-2q_u\cos 2(\xi-\xi_0)\right]u(\xi)=0 \qquad \text{(with } u=x, \text{ or } y\text{)}. \tag{3.2.9}$$

It is obvious that the subtraction of the initial phase constant ξ_0 from the variable ξ does not disturb any derivation of the above equation. This Mathieu equation can be solved exactly as mentioned in Section 3.1, and stable ion trajectories in RF-QMF are strictly obtained. In this case Mathieu stability regions in x- and y-directions are displayed in Figs.3-3(a) and (b), respectively. The stability region in the x-direction is identical with those in Fig.3-1 according to the definition of the parameter a_x in eq.(3.2.7). The parameter q_x has a positive sign from eq.(3.2.8). On the other hand, the signs of parameters in the y-direction are $a_y<0$ and $q_y<0$ from the definitions by eqs.(3.2.7) and (3.2.8). The stability region in the y-direction consists of the areas enclosed by the dotted lines as shown in Fig.3-3(b). As mentioned in Section 3.1, the stability region is symmetric about the q_u axis. The stability region in y-direction, therefore, is obtained in $a_x-q_x(>0)$ coordinate system by inverting the areas enclosed by the dotted lines of Fig.3-3(b) with respect to the q_x axis.

In order that ions injected into the two-dimensional quadrupole field survive until they reach the ion detector, ion trajectories must be stable in both x- and y-directions. Therefore, the stability diagram of RF-QMF is obtainable by overlapping Fig.3-3(b) onto Fig.3-3(a) as done in Fig.3-4. The overlapping region for stability is symmetric with respect to the q_x axis (see the inset of Fig.3-4). For an ion with positive charge q and mass m, the adjustment of V_{RF} determines q_x so as to take a value on the q_x axis in the stability region (see $\hat{q}_x$ in the inset). The point marked by an open circle in the inset of Fig.3-4 is assumed to have coordinates ($\hat{a}_x$, $\hat{q}_x$) in the a_x-q_x plane. The value of $\hat{a}_x$ in the stability region can be obtained by adjusting U in positive DC voltages (see eq.(3.2.7)). The motion of the ion of which mass m corresponds to the above $\hat{a}_x$ and $\hat{q}_x$ values is then stable in the x-direction.

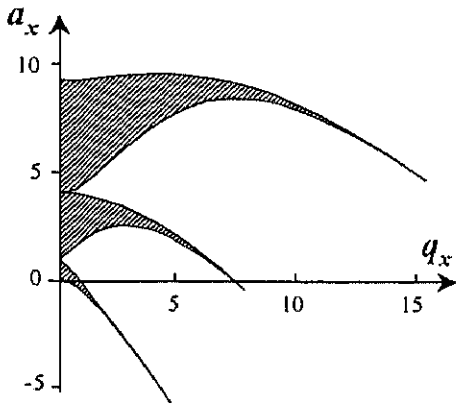

Fig.3-3(a) Mathieu stability diagram for the ion trajectory in x-direction.

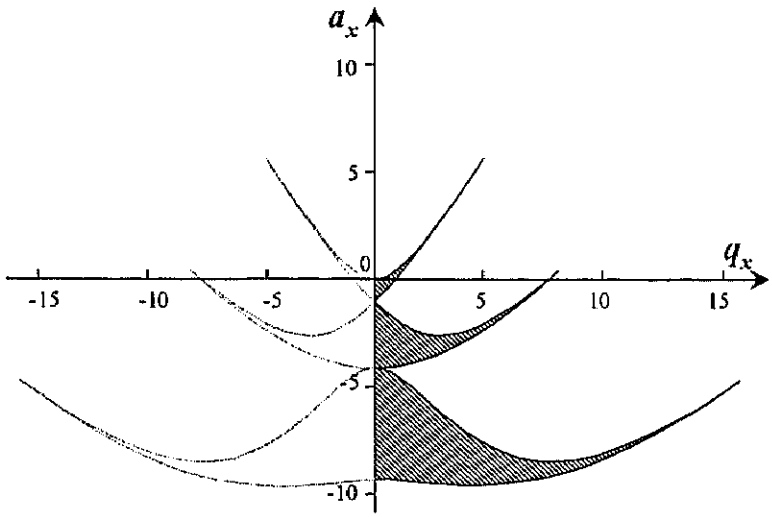

Fig.3-3(b) Mathieu stability diagram for the ion trajectory in y-direction in a_x-q_x coordinate system.

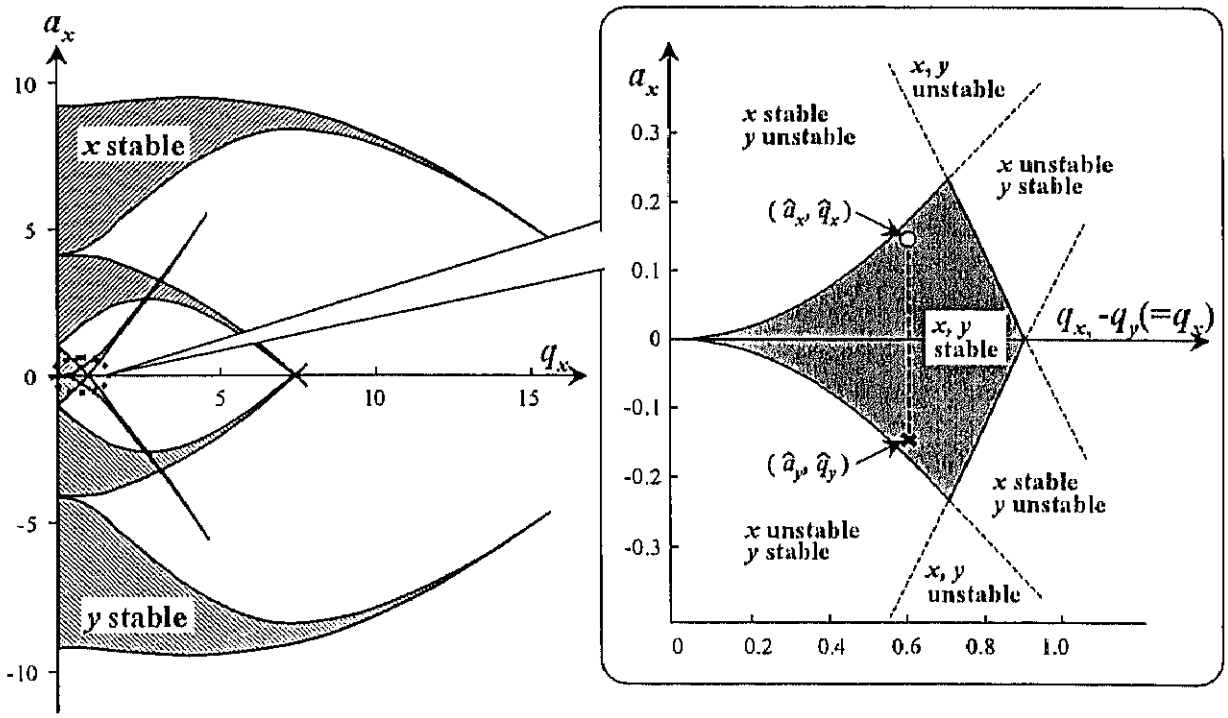

Fig.3-4 Mathieu stability diagram in two dimensions (x and y).

Similarly, the point marked by an x in the inset of Fig.3-4 is assumed to have coordinates ($\hat{a}_y$, $\hat{q}_x$) in a_x - q_x plane. The value of q_x gives q_y from the relation of q_x = - q_y in eq.(3.2.8). The parameter $\hat{a}_y$ lies at the symmetric position with $\hat{a}_x$, since it is negative but the absolute value remains unchanged from eq.(3.2.7). The motion of the ion which is stable in x-direction is thus stable in y-direction also.

The stable ion trajectory is obtained from eq.(3.1.11) with the replacement of ξ and β by $\Omega t/2$ and β_u. It is expressed in the following form:

$$u(t) = \mathrm{A}\sum_{n=-\infty}^{n=\infty} \mathrm{C}_{2n} \cos \omega_{un} t + \mathrm{B}\sum_{n=-\infty}^{n=\infty} \mathrm{C}_{2n} \sin \omega_{un} t \qquad (u(t)=x(t),\ y(t))\ , \qquad (3.2.10)$$

where ω_{un} is defined by

$$\omega_{un} = \frac{\Omega}{2}(2n + \beta_u) \qquad (u=x,\ y)\ . \qquad (3.2.11)$$

The value of β_u can be obtained from eq.(3.1.9) by putting μ equal to $i\beta$. The approximate solution of this algebraic equation is derived by Caricco[26] as follows:

$$\beta_u = \left[a_u - \frac{(a_u - 1)q_u^{\,2}}{2(a_u - 1)^2 - q_u^{\,2}} - \frac{(5a_u + 7)q_u^{\,4}}{32(a_u - 1)^3(a_u - 4)} - \frac{(9a_u^{\,2} + 58a_u + 29)q_u^{\,6}}{64(a_u - 1)^5(a_u - 4)(a_u - 9)} \right]^{1/2} . \qquad (3.2.12)$$

This formula and eq.(3.2.11) imply that ions travelling through RF-QMF oscillate with angular frequencies depending on their mass according to the values of a_u and q_u in the stable region.

3.2.2 Operation and mass separation in RF-QMF

The mass of ions which pass through RF-QMF all the way along four rod electrode is determined by setting the voltages U and V_{RF} in such a way that the parameters a_u and q_u corresponding to these voltages remain in the stability region. Although the parameters a_u and q_u

are not fully independent, they satisfy a linear relationship. From eqs.(3.2.7) and (3.2.8), this relationship is written as

$$\frac{a_x}{q_x} = \frac{-a_y}{-q_y} = \frac{2U}{V_{RF}} \quad . \tag{3.2.13}$$

Equation (3.2.13) is graphically expressed by a straight line on the a_u and q_u plane. If this line crosses the stability region, the points of (a_u, q_u) on the partial segment of the line cut off by the stability region provide a_u and q_u for stable ion motions. In x-direction, the partial segment of the line lies in the upper half of the stability region divided by q_x axis in the inset of Fig.3-4. The segment for y-direction lies in the lower half of the stability region in the same inset. However, we may discuss mass separation in RF-QMF using only the upper half of the stability diagram as shown in Fig.3-5. This is based on the fact that the absolute values of a_u and q_u are identical in both x- and y-directions and the stability regions for x- and y-directions are symmetric with respect to the q_x axis. The straight line derived from eq.(3.2.13) is named the operation line.

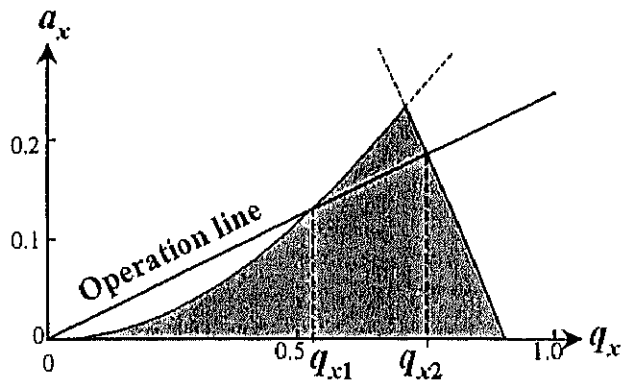

Fig.3-5 The operation line of RF-QMF.

As shown in Fig.3-5, if we tentatively assume the points of intersection on the operation line at the boundary of the stability region to be q_{x1} and q_{x2}, the ions with m/q in the range of

$$\left(\frac{4V_{RF}}{\Omega^2 r_0^2 q_{x2}}\right) = \frac{m_2}{q} \le \frac{m}{q} \le \frac{m_1}{q} = \left(\frac{4V_{RF}}{\Omega^2 r_0^2 q_{x1}}\right) \tag{3.2.14}$$

are successfully transmitted through RF-QMF to the detector. The slope of the operation line is determined in accordance with the ratio of U/V_{RF}. To obtain higher mass resolutions, therefore, the ratio of U/V_{RF} must be adjusted in such a manner that the operation line crosses the stability region near its tip. Writing this ratio as $(U/V_{RF})_{tip}$, we can observe a mass spectrum for a certain range of mass numbers by scanning the voltages U and V_{RF} under the condition of the constant ratio of $(U/V_{RF})_{tip}$ as shown in Fig. 3-6.

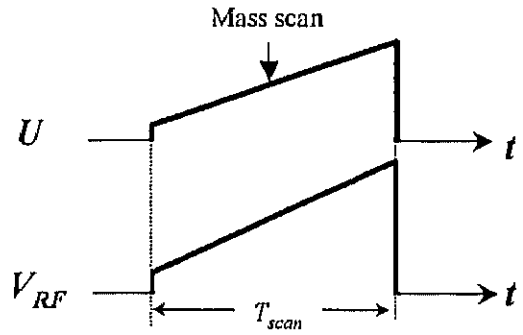

Fig.3-6 Typical operation sequence of RF-QMF. The mass-to-charge ratio of ions which transmit the RF-QMF can be changed by scanning the values of U and V_{RF} with maintaining a constant ratio U/V_{RF}.

3.2.3 Practical limits of the mathematical method

The mass separation described in the proceeding subsection is valid for an ideal quadrupole field over the whole range of four rods along the z-axis. The voltages of U and V_{RF} and angular frequency Ω are also assumed to be ideal in their absolute values and stability. Furthermore, the quadrupole field is assumed to have a sharp cut-off boundary in z-direction.

However, RF-QMF usually employs four rods with a circular cross section in actual instruments because of the difficulty in machining hyperbolic electrodes. In addition to this approximated shape of the electrodes, the quadrupole field is inevitably distorted by the error of

positioning of four rods in the mechanical construction. The sharp cut-off approximation must be modified by introducing a fringing field. Consequently, the stability diagram of the practical RF-QMF is no longer identical along z-direction, but has some diffusion near its edge. All of these factors result in a practical limit of the mass resolution of RF-QMF.

It is very difficult to examine these complicated factors in terms of mathematical analyses. Instead, a numerical simulation by means of a computer would be a powerful, or at least complementary tool for investigations of various characteristics of RF-QMF.

3.3 Ion trap mass spectrometer

Mass spectrometry with ITMS is usually performed in the following steps: (1) the ionization of atoms or molecules; (2) the confinement of all ion species in a three-dimensional trapping field; and (3) the extraction of a selected ion species by resonant forced oscillation. The most attractive feature of ITMS is that the distance from the ion detector to the position where ions are stored is much shorter than that of other types of mass spectrometers. Accordingly, ITMS is expected to provide a compact, low cost and highly sensitive mass spectrometer.

3.3.1 Description of the three-dimensional quadrupole field

ITMS employs a three-dimensional electric quadrupole field. The three-dimensional electric field is greatly simplified if we assume that it has axial symmetry around the z-axis and the reflection symmetry with respect to the z =0 plane. The electric field in charge-free space is derived from the potential Φ which obeys the Laplace equation:

$$\nabla^2\Phi = 0 \qquad (3.3.1)$$

Since the potential Φ is assumed to be axially symmetric, the general solution is written as

$$\Phi(r_p,\theta)=\sum_{l=0}^{\infty}\left[A_l r_p^{\ l}+B_l r_p^{\ -(l+1)}\right]P_l(\cos\theta) \qquad (3.3.2)$$

in spherical coordinates[27]. The functions $P_l(\cos\theta)$ are Legendre polynomials. Since our purpose is to find an ion trapping field in ITMS, we may assume that the above potential should be regular at the origin r_p=0. The coefficients B_l in this case can be set to null for all values of l. If we further confine ourselves for the above expansion to monopole, dipole and quadrupole terms, the potential Φ reduces to

$$\Phi(r_p,\theta)=A_0+A_1 r_p P_1(\cos\theta)+A_2 r_p^{\ 2}P_2(\cos\theta)$$

$$=A_0+A_1 r_p P_1(\cos\theta)+\frac{1}{2}A_2 r_p^{\ 2}(3\cos^2\theta-1).$$

The dipole term may be dropped because of the assumed reflection symmetry. Thus, the potential Φ can be expressed as

$$\Phi(r,\theta)=A_0+\frac{1}{2}A_2 r_p^{\ 2}(3\cos^2\theta-1). \qquad (3.3.3)$$

Here, we changed the coordinate system from spherical to cylindrical coordinate system, and noted the relations of $r_p\cos\theta=z$ and $r_p^{\ 2}=r^2+z^2$.

The two coefficients A_0 and A_2 are determined from boundary conditions. The curve of an equipotential surface with a value of Φ in the r-z plane is given by

$$z^2=\frac{1}{2}\left[r^2+\frac{2(\Phi-A_0)}{A_2}\right] \qquad (3.3.4)$$

from eq.(3.3.3). From the dimension analysis, the second term in the square brackets of eq.(3.3.4) can be replaced by the square of a constant radial coordinate r_0 as follows:

$$\frac{2(\Phi-A_0)}{A_2}=\pm r_0^{\ 2}\ . \qquad (3.3.5)$$

We take an equipotential surface with a value of $\Phi=\Phi_0$ corresponding to $-r_0^2$ in the above formula. Another equipotential surface with a value of $\Phi=0$ is taken for $+r_0^2$. Then, the coefficients A_0 and A_2 are determined to be $\Phi_0/2$ and $-(\Phi_0/r_0^2)$, respectively. Thus, the potential $\Phi(r,z)$ given by eq.(3.3.3) results in the following form:

$$\Phi(r,z)=\frac{\Phi_0}{2}+\frac{\Phi_0}{2r_0^2}(r^2-2z^2). \tag{3.3.6}$$

The curve of the equipotential surface with a value of Φ_0 is given by

$$z=\pm\sqrt{\frac{1}{2}(r^2-r_0^2)} \tag{3.3.7}$$

in the r-z plane. Another curve of the equipotential surface with a value of $\Phi=0$ is determined by

$$z=\pm\sqrt{\frac{1}{2}(r^2+r_0^2)}\ . \tag{3.3.8}$$

The cross section of the axially symmetric equipotential surface at an arbitrary azimuthal angle is drawn in Fig.3-7.

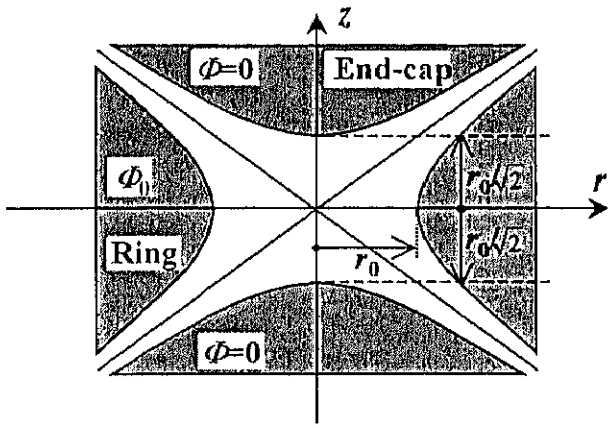

Fig.3-7 The cross section of the axially symmetric equipotential surface between the end-cap and ring electrodes at an arbitrary azimuthal angle.

From these results, the configuration of electrodes to generate a three-dimensional quadrupole field for ITMS is determined. As was shown in Fig. 2-5(b), ITMS is comprised of one ring

electrode and two end-cap electrodes. The cross section of these electrodes cut by a plane including the z-axis should be shaped as shown in Fig.3-7. The inner surface of the ring electrode should be machined according to eq.(3.3.7). Its inner radius is r_0. The surfaces of the end-cap electrodes should have the shape given by eq.(3.3.8). The separation between the two end-cap electrodes is $r_0/\sqrt{2}$.

The electric field components in ITMS are easily obtained from the potential given by eq.(3.3.6). The explicit forms are

$$E_r = -\frac{\partial \Phi(r,z)}{\partial r} = -\frac{\Phi_0}{r_0^2} r \tag{3.3.9}$$

and

$$E_z = -\frac{\partial \Phi(r,z)}{\partial z} = 2\frac{\Phi_0}{r_0^2} z \ . \tag{3.3.10}$$

3.3.2 Equations of ion motion

The equations of ion motion in the cylindrical coordinates (r, ϕ, z) are as follows:

$$m\left\{\frac{d^2 r(t)}{dt^2} - r\left(\frac{d\phi(t)}{dt}\right)^2\right\} = qE_r, \tag{3.3.11a}$$

$$m\left\{2\frac{dr(t)}{dt}\frac{d\phi(t)}{dt} + r\frac{d^2\phi(t)}{dt^2}\right\} = m\frac{1}{r}\frac{d}{dt}\left\{r^2\frac{d\phi(t)}{dt^2}\right\} = qE_\phi = 0, \tag{3.3.11b}$$

and

$$m\frac{d^2 z(t)}{dt^2} = qE_z. \tag{3.3.11c}$$

Since the electric field is axially symmetric around z axis, we put E_ϕ=0. From the second equation, we obtain immediately $r^2(d\phi(t)/dt)$=const. This is an expression of the conservation of

angular momentum of ions. For ion motions in ITMS, we may assume this constant to be zero for simplicity. In this case, the equations of the ion motion reduce to the following simple forms:

$$m\frac{d^2r(t)}{dt^2} = qE_r = -q\frac{\Phi_0}{r_0^2}r, \tag{3.3.12a}$$

and

$$m\frac{d^2z(t)}{dt^2} = qE_z = 2q\frac{\Phi_0}{r_0^2}z. \tag{3.3.12b}$$

The electric potential Φ_0 can be taken, in general, to be a superposition of DC voltage of U and RF voltage of $V_{RF}\cos\Omega t$ in ITMS also. It is convenient to add U in deriving the Mathieu equation for ion motions. With the transformation of $\Omega t=2\xi$ defined by eq.(3.2.5), the above equations are modified to

$$\frac{d^2r(\xi)}{d\xi^2} + \frac{4q}{m\Omega^2r_0^2}\left[U + V_{RF}\cos 2(\xi-\xi_0)\right]r(\xi) = 0 \tag{3.3.13a}$$

and

$$\frac{d^2z(\xi)}{d\xi^2} - \frac{8q}{m\Omega^2r_0^2}\left[U + V_{RF}\cos 2(\xi-\xi_0)\right]r(\xi) = 0. \tag{3.3.13b}$$

The ion motions in r- and z-directions, therefore, are described by the Mathieu equation in the form of eq.(3.1.1). The two parameters of a_u and q_u with $u = r$ or $u = z$ are defined in the following manner:

$$a_z = -2a_r = -\frac{8qU}{m\Omega^2r_0^2} \tag{3.2.14a}$$

and

$$q_z = -2q_r = \frac{4qV_{RF}}{m\Omega^2r_0^2}. \tag{3.2.14b}$$

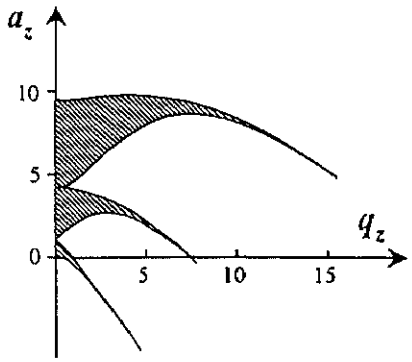

Fig.3-8(a) Mathieu stability diagram for the ion trajectory in the z-direction.

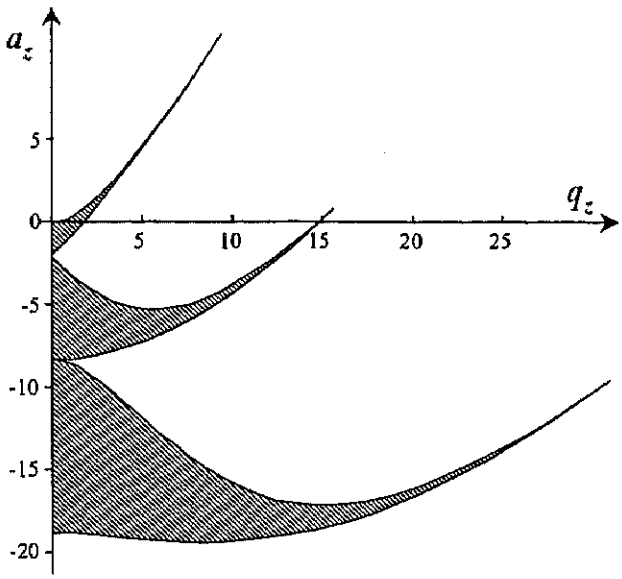

Fig.3-8(b) Mathieu stability diagram for the ion trajectory in the r-direction in a_z-q_z coordinate system.

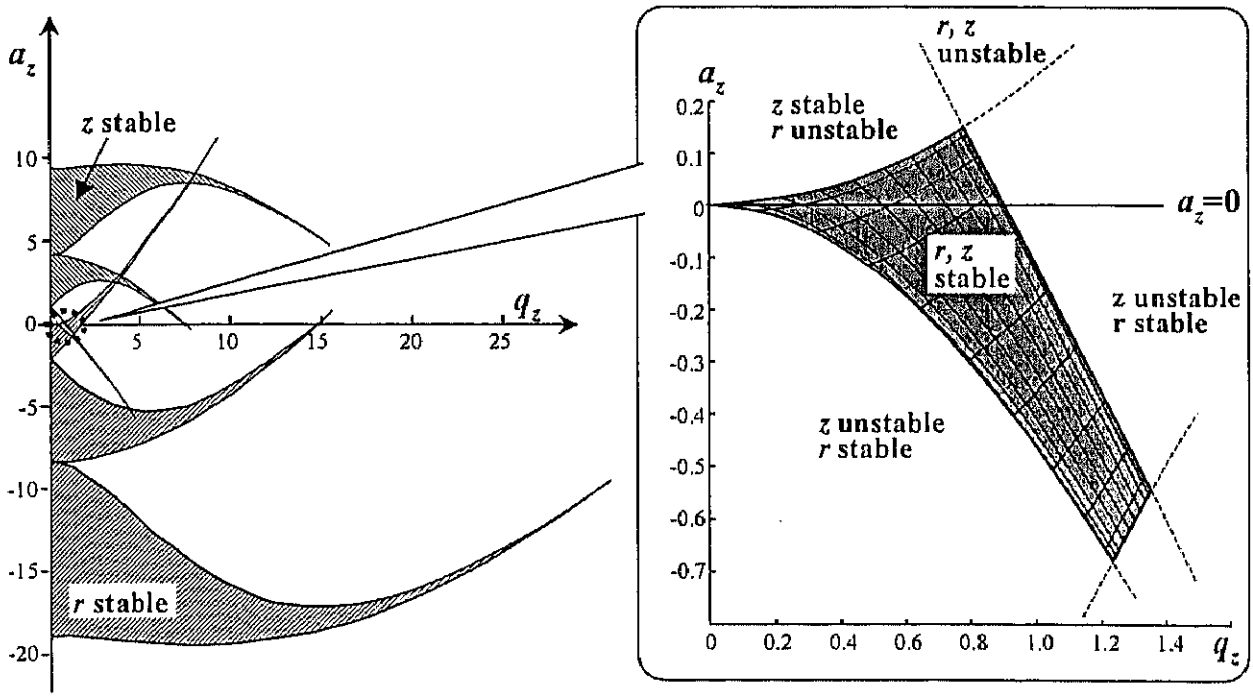

Fig.3-8(c) Mathieu stability diagram for the ITMS.

Thus, the stability parameters of a_u and q_u for the z- and r-directions differ by a factor of –2 in ITMS, although the absolute values of a_u and q_u in RF-QMF are identical in both x- and y-directions. In the case of $U<0$ and $V_{RF}>0$, the stability region in z-direction is obtained as

displayed in Fig.3-8(a). On the other hand, Fig.3-8(b) shows the stability region in r-direction, that is a plot in the a_z-q_z coordinate system not in a_r-q_r. Stability regions in both r- and z-directions are the areas as indicated in Fig.3-1, respectively. However, the parameters of a_u and q_u for the z- and r-directions differ by a factor of –2 from eqs.(3.2.14a) and (3.2.14b). The stability region in the r-direction must be twice the size of that in z-direction with an opposite sign. The stability region of ITMS, therefore, is obtained by overlapping the stability regions in the two directions (r, z) of ion motions as shown in Fig.3-8(c). Only the ions having a_u and q_u in this stability region stay in a limited space in ITMS with their characteristic stable oscillations.

3.3.3 Stable ion oscillations in ITMS

For the values of a_u and q_u in the stability region, a stable ion trajectory is given by the same expression as RF-QMF which was derived as eq.(3.2.10) with the definition of eq.(3.2.11). For clarity we write it again for ITMS, *i.e.*

$$u(t) = \mathrm{A}\sum_{n=-\infty}^{n=\infty} \mathrm{C}_{2n} \cos\omega_{un} t + \mathrm{B}\sum_{n=-\infty}^{n=\infty} \mathrm{C}_{2n} \sin\omega_{un} t \quad (u = r \text{ or } z) \tag{3.3.15}$$

where

$$\omega_{un} = \frac{\Omega}{2}(2n + \beta_u) \qquad (u = r \text{ or } z). \tag{3.3.16}$$

In a usual operation of ITMS, only the RF voltage is applied to the ring electrode. This means that we may put U=0 which makes the parameter a_z =0 from eq.(3.14a). Hence, all ions having q_z on the line of a_z =0 in the stability diagram are stably oscillating in ITMS.

We consider ion motions in the z direction at first. The angular frequency ω_{zn} depends on a_z and q_z through the value of β_z as expressed by eq.(3.2.12). As already described regarding the general solution of the Mathieu equation, the amplitudes C_{2n} in eq.(3.3.15) also depend on a_u and

q_u in ITMS. The dependence is more important in ITMS than in RF-QMF. The approximate formulas derived by Carrico[26] are

$$\frac{C_{2n}}{C_{2n-2}} = \frac{-q_u}{(2n+\beta_u)^2\left(1-\dfrac{a_u}{(2n+\beta_u)^2}-\dfrac{q_u^{\,2}}{(2n+\beta_u)^2(2n+2+\beta_u)^2(1-\cdots\text{etc.}}\right.} \qquad (3.3.17)$$

and

$$\frac{C_{2n}}{C_{2n+2}} = \frac{-q_u}{(2n\text{-}2+\beta_u)^2\left(1-\dfrac{a_u}{(2n+\beta_u)^2}-\dfrac{q_u^{\,2}}{(2n+\beta_u)^2(2n-2+\beta_u)^2(1-\cdots\text{etc.}}\right.} \quad . \qquad (3.3.18)$$

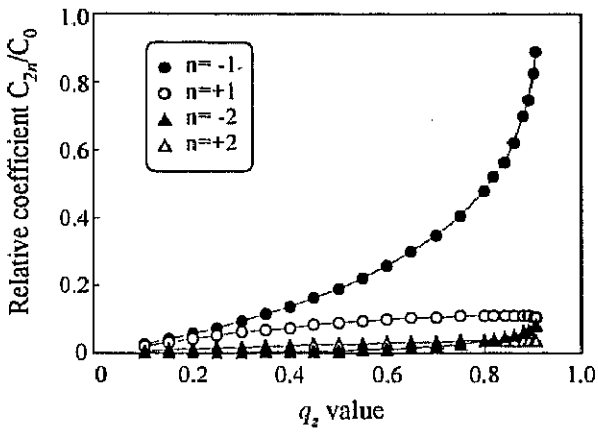

Fig.3-9 The dependence of q_z on the calculated coefficients C_{2n} of the n-th oscillation in comparison with that of the n=0 (fundamental) oscillation.

The value of C_0 is largest over the entire range of $0 \leq q_z \leq 0.908$ in the stability region. The ratios of C_{2n}/C_0 calculated from eqs.(3.3.17) and (3.3.18) by putting $a_z = 0$ are plotted in Fig.3-9 as a function of q_z for $n=\pm 1$ and for $n=\pm 2$. It is obvious from this graph that the amplitudes other than $n=0$ are sufficiently small as compared to C_0 in the range of $q_z \leq 0.4$. In other words, the $n=0$ oscillation mode is dominant in the operating condition with $a_z = 0$. Therefore, the ion motions in z-direction can be expressed in the following simple harmonic oscillation to a good approximation;

$$z(t) \approx \mathrm{A}_z \cos(\omega_{z0} t + \phi_0) \qquad (\text{for } q \leq 0.4) \qquad (3.3.19)$$

with

$$\omega_{z0} = \beta_z \frac{\Omega}{2} . \qquad (3.3.20)$$

The description of ion motions in r-direction is completely analogous to that in z direction. From eq.(3.3.14a), the parameter a_r is automatically null in the operating condition of a_z =0 for z-direction, since U=0. The value of C_0 and the ratios of C_{2n}/C_0 for a_r =0 are calculable in a similar manner as for z-direction. If we note the relation of $q_r = q_z/2$, dominance of C_0 is obvious. Thus, the n=0 oscillation mode is dominant in r-direction also. The ion motion in r-direction is given by

$$r(t) \approx \mathrm{A}_r \cos(\omega_{r0} t + \phi_0') , \qquad (3.3.21)$$

with

$$\omega_{r0} = \beta_r \frac{\Omega}{2} . \qquad (3.3.22)$$

In a rougher approximation than that in eq.(3.2.12), the value of β_u can be expressed as

$$\beta_u \sim q_u / \sqrt{2} . \qquad (3.3.23)$$

Therefore, the angular frequency ω_{r0} of r direction becomes about half of ω_{z0} form the relation of $q_r = q_z/2$. Ions in ITMS oscillate at lower frequencies in r direction in comparison with z direction. An example of the stable oscillations in ITMS is presented in Fig.3-10.

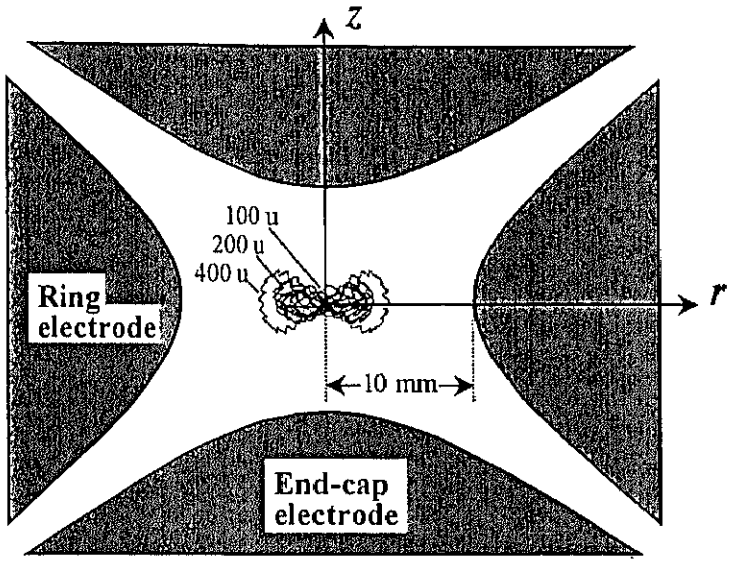

Fig.3-10 The trajectories of m=100, 200 and 400 u ions in ITMS, when RF voltage $V_{RF}\cos\Omega t$ (V_{RF}=600V, $\Omega/2\pi$=909 kHz) is applied to the ring electrode. The ions all oscillate stably with different frequencies according to their masses.

3.3.4 Operation and mass separation in ITMS

As described in the proceeding section, the first step in mass spectroscopy with ITMS is the injection of ions under the condition of U=0(a_z=0) and an RF voltage application to give relatively small q_z values. After injecting ions, all ions having q_z on the line of a_z =0 in the stability diagram continue their stable oscillations mainly in the fundamental mode in both r- and z-directions. The space where ions are moving is confined in a small region near the center of ITMS. This is the second step of operation of ITMS, and it is called the ion trapping step.

The final step is to extract a specific ion by applying an auxiliary RF voltage of $V_{res}\cos\omega_{res}t$ on the end-cap electrodes in dipolar fashion. From eqs.(3.3.23) and (3.2.14b) the angular frequency ω_{z0} of the fundamental oscillation, that is expressed in eq.(3.3.20), can be rewritten as

$$\omega_{z0} \approx q_z \frac{\Omega}{2\sqrt{2}} = \frac{\sqrt{2}qV_{RF}}{mr_0^2\Omega}. \qquad (3.3.24)$$

Thus, ions oscillate with different angular frequencies according to their masses. When a specific ion moves with the angular frequency agreeing with that of the auxiliary RF voltage ($\omega_0=\omega_{res}$), the amplitude of the oscillation in z-direction increases selectively due to the resonant forced oscillation. This process is analogous to ICR-MS. The frequency of the fundamental oscillation of trapped ions corresponds to the cyclotron frequency, while the auxiliary RF voltage works like the excitation pulse in ICR-MS. As an example, the oscillations of several ion species having different fundamental frequencies are shown in Fig.3-11.

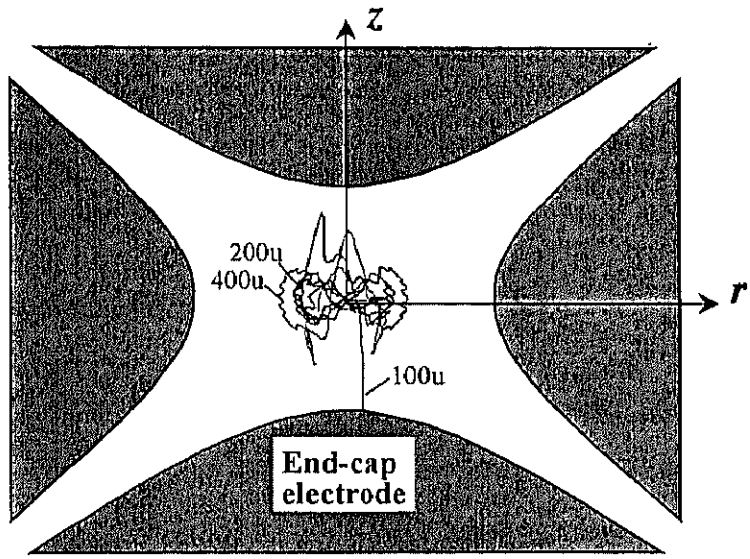

Fig.3-11 The trajectories of m=100, 200 and 400 u ions in ITMS, when RF voltage $V_{RF}\cos\Omega t$ (V_{RF}=600V, $\Omega/2\pi$=909kHz) to the ring electrode and resonance voltage $\pm V_{res}\cos\omega_{res}t$ (V_{res}=10V, $\omega_{res}/2\pi$= 260.7kHz) to the end-cap electrodes are applied. Only m=100[u] ion whose oscillation frequency agrees with that of the resonance field become excited to reach one of the end-cap electrodes.

Only one ion species, the angular frequency of which agrees with that of the resonance field, is resonated with the auxiliary RF voltage. Finally the excited ions which reach the aperture on one of the end cap electrodes are detected by a detector as shown in Fig.2-5(b). A mass spectrum in a certain range of mass numbers is observed by scanning the mass m of the selected ion; this is called *mass-selective instability scanning*.

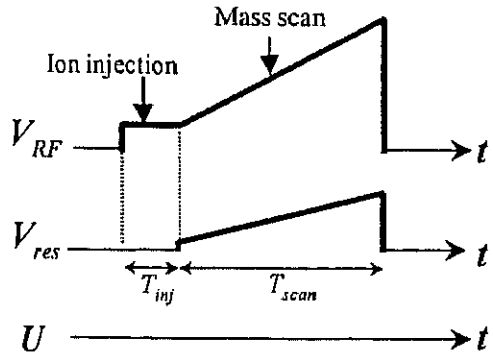

Fig.3-12 Typical operation sequence of ITMS. In the period of T_{inj}, atoms or molecules in a specimen are ionized and trapped in ITMS. In the period T_{scan}, the mass-to-charge ratio of ions can be scanned by varying the amplitude of RF voltage V_{RF}.

Equation (3.3.24) shows the *mass-selective instability scanning* is usually carried out by changing the magnitude of V_{RF} with a fixed auxiliary RF voltage V_{res}. Fig.3-12 is a conceptual drawing of mass spectroscopy with ITMS.

3.3.5 Primary factors relevant to the performance

Many factors must be examined to understand the motions of ions in ITMS and to improve the performance. Which factor has a strong correlation with what performance item is summarized in Table 3-1. Mathematically rigorous theories could of course be developed to estimate the contribution of each factor to the performance. As mentioned for RF-QMS, however, it is important to develop a method of computer simulation which is able to treat some realistic conditions like collisions with ion buffering gas atoms. It should be emphasized that the computer simulation is suitable for quick empirical estimates of performance while changing various parameters.

Table 3-1. Primary factors relevant to the performance of ITMS

ITMS parameters	Performance		
	Mass resolution (FWHM)	Mass accuracy (shifting degree)	Sensitivity
He gas pressure	○	○	
Space charge	○	○	○
Mass analysis scanning method	○	○	
Resonance voltage	○	○	○
Injection method			○
Electrode structure (shape, configuration)	○	○	○

○ : strong correlation